SOLUTION MINING RESEARCH INSTITUTE
679 Plank Road
Clifton Park, NY 12065, USA

Telephone: +1 518-579-6587
www.solutionmining.org

Technical Conference Paper

1965 – 2025

Novel Approach to Conducting a Mechanical Integrity Test with Optical Fiber

Brandon Lampe[1], Timothy Lynn[1], Lafe Windmiller[2], and Kassie Mobley[2]

[1] *Agapito Associates, Grand Junction, Colorado, USA*
[2] *Enbridge, Houston, Texas, USA*

SMRI Fall 2025 Technical Conference
29 - 30 September 2025
Wichita, Kansas, United States

Solution Mining Research Institute Fall 2025 Technical Conference

Wichita, Kansas, United States 29 - 30 September 2025

Novel Approach to Conducting a Mechanical Integrity Test with Optical Fiber

Brandon Lampe[1], Timothy Lynn[1], Lafe Windmiller[2], and Kassie Mobley[2]

[1] *Agapito Associates, Grand Junction, Colorado, USA*
[2] *Enbridge, Houston, Texas, USA*

Abstract

Accurate assessments of cavern integrity are necessary to ensure the fluids contained within a cavern do not contaminate the external environment. The basic results from a mechanical integrity test (MIT) are that of leak rate from a cavern and the associated precision or accuracy. The industry standard for evaluating cavern integrity is the nitrogen-brine interface MIT [1]. However, many variants to this approach are routinely implemented, which commonly use different test fluids and approaches for calculating leak rate.

Typical MITs are based on data acquired at two points in time, and the leak rate is determined from the change of test-fluid volume. Recent advances in sensing technology allow for acquisition of distributed down-hole temperature using optical fiber. The use of optical fiber allows for acquisition of down-hole temperature, from surface to total depth, almost instantly and at high sample rates (e.g., 10 full temperature logs per hour). The implementation of optical fiber during an MIT allows for stochastic techniques to determine the leak rate and the associated accuracy.

This paper discusses a novel approach for determining the leak rate and associated accuracy during an MIT of a solution-mined cavern. The large amount of acquired data allows for the leak rate and associated accuracy to be determined using stochastic methods, and a theory for this approach is provided. Optical fiber has been used in numerous MITs, and a case study from an optical-fiber MIT on a gas-storage cavern located in Louisiana, USA, is presented.

Key Words: Mechanical Integrity Test (MIT), Optical Fiber, Gas Storage

1 Introduction

Typical mechanical integrity tests (MITs) on solution-mined caverns provide results in the form of (1) a leak rate and (2) the associated minimum detectable leak rate (MDLR). MITs are often completed with a gas (e.g., nitrogen) or a light hydrocarbon liquid as the test fluid. Further descriptions of related to the technique of conducting a nitrogen-brine interface MIT and others are provided by [1], [2], [3], and [4].

The analysis of an MIT results in a calculated leak rate (CLR), which is typically based on data acquired at two points in time (the start and end of logging runs). The MIT approach presented here utilizes optical fiber (OF) to acquire distributed down-hole temperature continuously during the MIT, and these data are used to determine the CLR along with the associated CLR accuracy. A fundamental difference in this technique is that the OF remains in the cavern over the duration of the MIT, and this allows for continuous down-hole temperature acquisition, from surface to total depth, during the MIT.

Two MIT scenarios are illustrated in Figure 1:

- (left) test-fluid interface is located in the uncased wellbore, and
- (right) test-fluid interface is located within the cavern interval.

The use of OF to acquire data during an MIT may be applied in both of these scenarios.

The paper provides a detailed description of the statistical theory used to develop the CLR and determine the accuracy of the CLR when conducting an MIT with OF. Following this, Section 3 presents a case study where OF was used to complete an MIT on a gas-filled storage cavern, and Section 4 provides a discussion on CLR accuracy.

2 Analysis Theory

The theory presented in this section will focus on the following:

1. Determining a CLR of gas from a storage system,
2. Calculating the accuracy of the CLR,
3. Determining if the CLR and the associated accuracy indicate a loss of gas from the storage system.

If the CLR and associated accuracy range encompasses zero (flow rate), the MIT will not have identified a loss or gain of gas during the MIT. However, if the CLR and associated accuracy range do not encompass zero, a loss or influx to the cavern will have been detected.

2.1 Density of Gas

The gas contained in the cased wellbore and uncased cavern interval will be considered during the evaluation of the storage system. To accurately determine the CLR, the density of gas with depth will be determined. The following equation will be used to determine the density of gas at discrete depths (*i*) during the MIT based on the measured pressure, temperature, and gas composition.

$$\rho_i = \frac{P_i}{R_{sp} T_i z_i} \tag{1}$$

where:

ρ_i: mass density of compressible gas at point *i*

P_i: absolute gas pressure at point *i*

R_{sp}: specific gas constant

T_i: absolute gas temperature at point *i*

z_i: compressibilty factor determined from equation of state at point *i*

This evaluation assumes the temperature data are acquired via optical fiber (OF) that is suspended along the wellbore axis, and the acquired temperature data are representative of all temperatures within the cavern at the associated depth. Down-hole pressure of the gas will be approximated from the measured wellhead pressure, measured down-hole temperature, and an equation of state for the specific composition of gas in the caverns.

2.2 Calculated Leak Rate

The calculated leak rate (CLR) will be based on the change in the volume of gas at standard conditions. A detailed description of the method used to determine down-hole pressure, gas volume at standard conditions, and the calculated leak rate are provided in the following subsections.

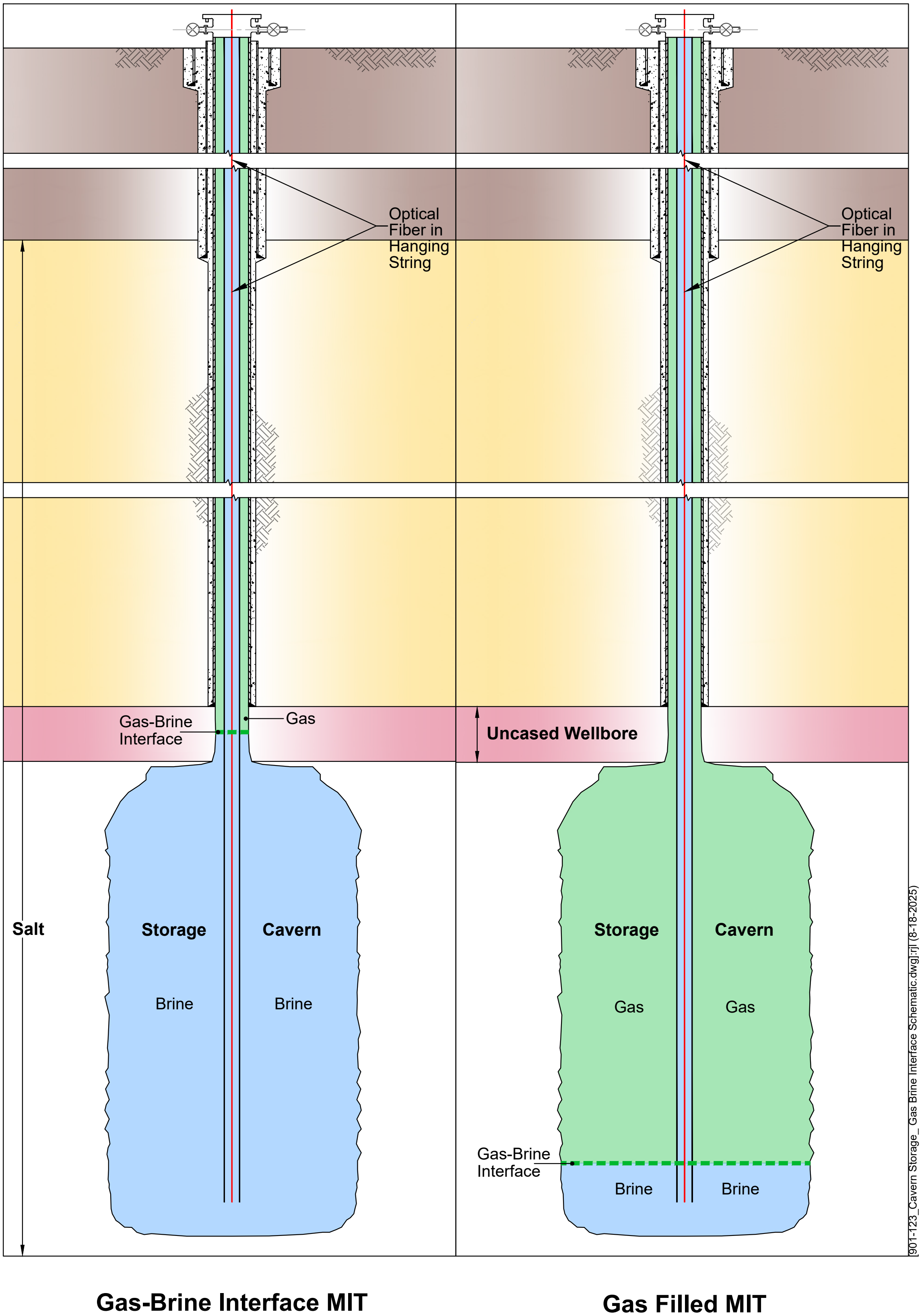

Figure 1: Illustration of the two common MIT scenarios.

2.2.1 Determination of Down-Hole Pressure

The down-hole pressure is determined by discretizing the wellbore into m vertical depth increments. Calculated pressure at the depth increment (i) is given by the following equation.

$$P_i = P_{i-1} + \sum_{i=1}^{m} \rho_i h_i \tag{2}$$

where:

P_i: Calculated gas pressure at depth i

P_{i-1}: Determined gas pressure at depth $i-1$

ρ_i: Calculated gas density at depth i

h_i: Height depth increment between point i and $i-1$

2.2.2 Determination of Gas Volume at Standard Conditions

The cumulative volume of gas in the storage system at standard conditions (e.g., temperature of 60 degrees Fahrenheit and pressure of 14.65 pounds per square inch absolute) will be determined at specific points in time. The wellbore and cavern will be vertical discretized into m depth increments, and the cumulative gas volume in the storage system at time j will be determined using Equation 3. The volume of gas at standard conditions will be determined at a set interval over the MIT duration based on the optimum data acquisition rate of the OF (approximately every 5 minutes).

$$V^j = \sum_{i=1}^{m} \left[v_i^j \left(\frac{\rho_i^j + \rho_{i-1}^j}{2\rho} \right) \right] \tag{3}$$

where:

V^j: cumulative measured gas volume in storage system (at standard conditions) at time j

v_i^j: physical gas volume associated with h_i at time j

ρ_{i-1}^j: physical gas density incremental down-hole gas volume at depth increment $i-1$

ρ: gas density at standard conditions

2.2.3 Determination of Calculated Leak Rate

Based on the measured volume of gas at time j, a best estimate of the true volume of gas with time will be referred to as $\hat{V}^j$, and the form of $\hat{V}^j$ is provided in Equation 4. An estimate of the error between the best estimate of the true volume of gas and the measured volume of gas in the storage system is provided by Equation 5.

$$\hat{V}^j = \beta_0 + \beta_1 t^j \tag{4}$$

where:

$\hat{V}^j$: best estimate (fit) of cumulative gas volume at time increment j

β_0: unknown scalar constant fitting parameter

β_1: unknown scalar constant parameter acting on time (t)

t^j: discrete point in time at increment j

$$\epsilon^j = V^j - \hat{V}^j \tag{5}$$

where:

ϵ^j: estimate of error between true and measured volume of gas

Estimates of the model parameters β_0 and β_1 will be determined by choosing values that minimize the residual (or error) between the measured cumulative gas inventory with time (V^j) and the linear model best fit $(\hat{V}^j)$, as shown in Equation 6.

$$\epsilon^j = V^j - (\beta_0 + \beta_1 t^j) \tag{6}$$

Where ϵ^j is the error between a measured gas volume and the model prediction. Variables β_0 and β_1 represent estimates of the unknown model parameters that may be determined by minimizing the sum of squares of the residuals, where the sum of squares of the residuals is given by Equation 7.

$$\|\epsilon\| \equiv \sum_{j=1}^{m} (\epsilon^j)^2 \tag{7}$$

Where m is the total number of times the gas inventory in the caverns will be determined (i.e., observations). An expression for the appropriate values of β_0 and β_1 that minimize $\|\epsilon\|$ may be obtained by solving the set of partial differential equations given by Equations 8 and 9.

$$\frac{\partial \|\epsilon\|}{\partial \beta_0} = 0 \tag{8}$$

$$\frac{\partial \|\epsilon\|}{\partial \beta_1} = 0 \tag{9}$$

The parameter β_1 represents the unknown relationship between cumulative gas inventory and time; therefore, this term directly represents the CLR, as shown in Equation 10

$$CLR = \beta_1 \tag{10}$$

2.2.4 Accuracy of the CLR

If the model residuals are uncorrelated and follow a normal distribution, the accuracy of the CLR may be calculated from an approximation of the unbiased variance (σ^2) in ϵ, as shown in Equation 11.

$$\sigma^2 = \frac{1}{m} \sum_{j=1}^{m} \left(\epsilon^j - \bar{\epsilon}\right)^2 \tag{11}$$

Where $\bar{\epsilon} = \frac{1}{m} \sum_{j=1}^{m} \epsilon^j$, is the mean residual value. The σ^2 may be implemented to compute the variance of β_1 as described in Equations 12.

$$Var(\beta_1) = \frac{\sigma^2}{\sum_{j=1}^{m} \left(t^j - \bar{t}\right)^2} \tag{12}$$

where:

$Var(\beta_1)$: the unbiased variance in the β_1 parameter

$\bar{t}$: mean time duration of the MIT

The mean time $(\bar{t})$ is defined as $\bar{t} = \frac{1}{m}\sum_{j=1}^{m} t^j$. The CLR is represented as β_1 and has units of volume per unit time (i.e., flow rate). The accuracy of the CLR may be determined from the standard error (SE) associated with the β_1, which is given in Equation 13.

$$SE = \sqrt{Var(\beta_1)} \tag{13}$$

The SE is used to calculate confidence interval of the CLR. Where within a 95% confidence interval range, there is a 95% probability the true unknown value of the CLR will be contained. Approximate expressions for the lower and upper bounds of the 95% confidence interval of the CLR $(CLR_{LB}$ and $CLR_{UB})$, are given by Equations 14 and 15, respectively.

$$CLR_{LB} = CLR - 2 \cdot SE(CLR) \tag{14}$$

$$CLR_{UB} = CLR + 2 \cdot SE(CLR) \tag{15}$$

The exact expression for the confidence interval of the CLR does not multiply the SE by a constant of 2; rather, this factor varies with the number of observations m and contains the 97.5% quantile of a t-distribution with $m-2$ degrees of freedom.

2.3 MIT Evaluation Criteria

The integrity of the storage system and lack of a significant leak will be assessed in terms of a CLR along with the lower and upper bounds of the 95% confidence interval of the CLR. Therefore, if the range between CLR_{LB} and CLR_{UB} contain zero, no leak will have been identified - this is expressed mathematically by Equation 16. However, if the range between CLR_{LB} and CLR_{UB} does not contain zero, a flow of gas will have been determined and further investigation is warranted.

$$\text{No detectible leak if:} \quad CLR_{LB} \leq 0 \leq CLR_{UB} \tag{16}$$

3 Case Study

The following section presents a case study where optical fiber was used to acquire continuous-distributed temperature during an MIT on a solution-mined cavern operated by Enbridge. The cavern is located in southern Louisiana and was full of natural gas during the four-day MIT in November of 2024.

3.1 Well and Cavern Completion Details

The cavern is completed with a 20-inch outside diameter (OD) production casing (0.508 m) that was set at a depth of 4,299 ft (1,310 m) relative to the bradenhead flange (bhf). A workover was completed prior to the MIT to satisfy the mandated 15-year casing inspection logging. All hanging strings were removed during the workover while the cavern remained gas-filled. Figure 2 illustrates the well completion prior to (left) and during the gas-filled MIT (right). Further details related to the removal of the hanging strings was provided by Nealy, Heath, and Mickelson [5].

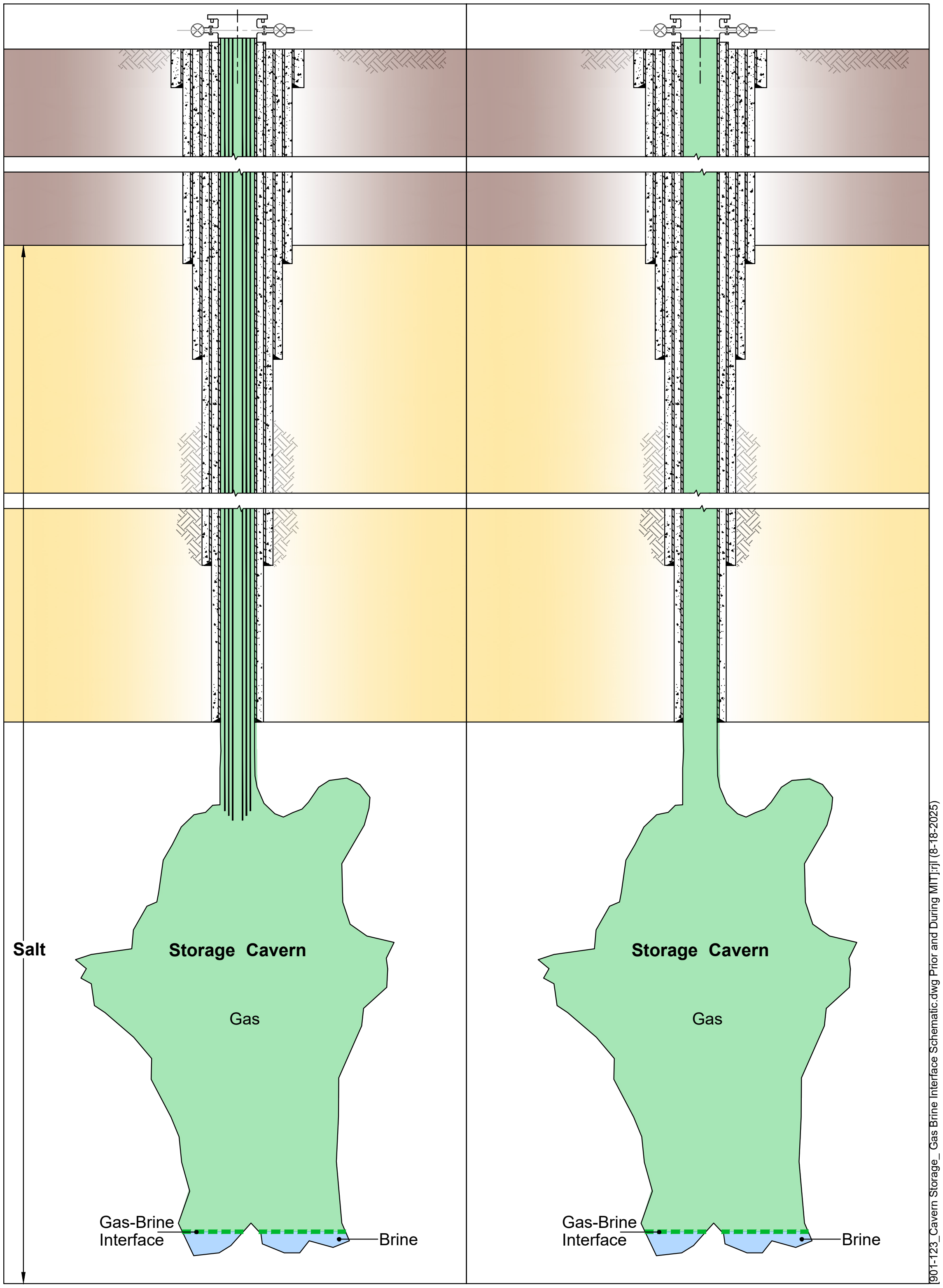

Prior to Workover **Configuration During MIT**

Figure 2: Illustration of the cavern completion prior to (left) and during (right) MIT.

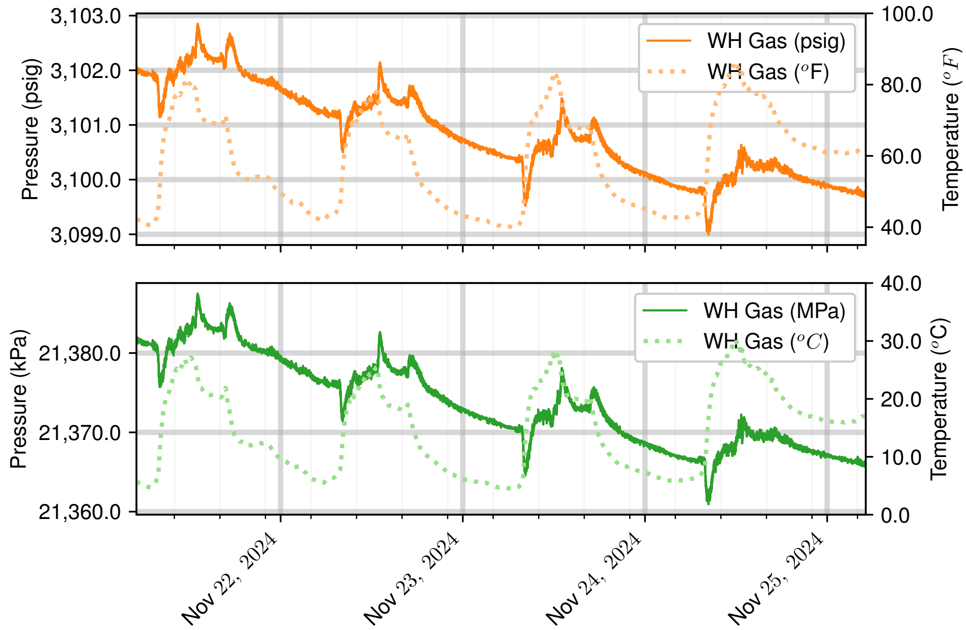

Figure 3: Surface pressure and temperature recorded during the MIT in US units (top) and SI units (bottom).

3.2 Acquired Data

A pressure-temperature-density log was run before the MIT to confirm the gas-brine interface depth, which was located at the cavern floor. Surface wellhead pressure and temperature were continuously measured during the MIT, and Figure 3 illustrates these values. Down-hole temperature data was continuously acquired during the MIT with distributed temperature sensing (DTS) OF. The down-hole temperature was calibrated to a memory gauge affixed to the lower end of the fiber line. Distributed temperature was acquired approximately every five minutes during the MIT, which results in 1,343 temperature logs. Figure 4 illustrates the measured down-hole temperature and temperature change during the MIT.

3.3 Cavern Volume

The physical volume occupied by gas in the cavern was approximated from (1) the cased-well geometry and (2) the most recent sonar caliper survey in the uncased portion of the cavern. A summary of the most recent sonar survey is provided in Table 1, and orthogonal cross sections from the sonar survey are provided in Figure 5.

Table 1: Summary of the cavern data.

Sonar Parameter	Parameter Value	
	US Units	SI Units
Sonar Date	December 2, 2023	
Cemented Casing Depth	4,299 ft bhf	1,310 m bhf
Sonar Volume	6,226 MMB	9.90(10^6) m^3
Sonar Total Depth	5,239 ft bhf	1,597 m bhf

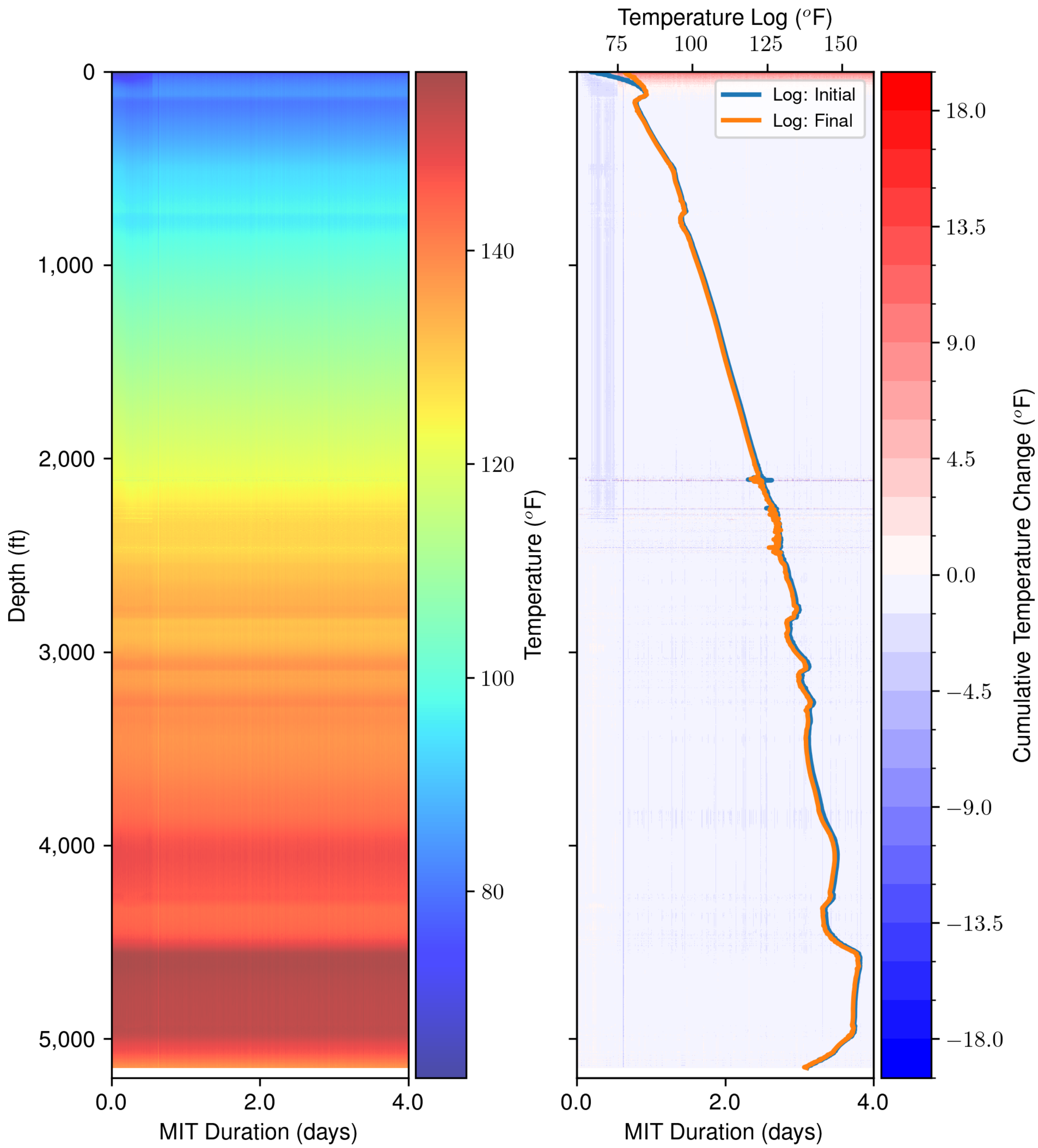

Figure 4: Illustration of the 1,343 down-hole temperature logs (left) and cumulative change during the MIT (right).

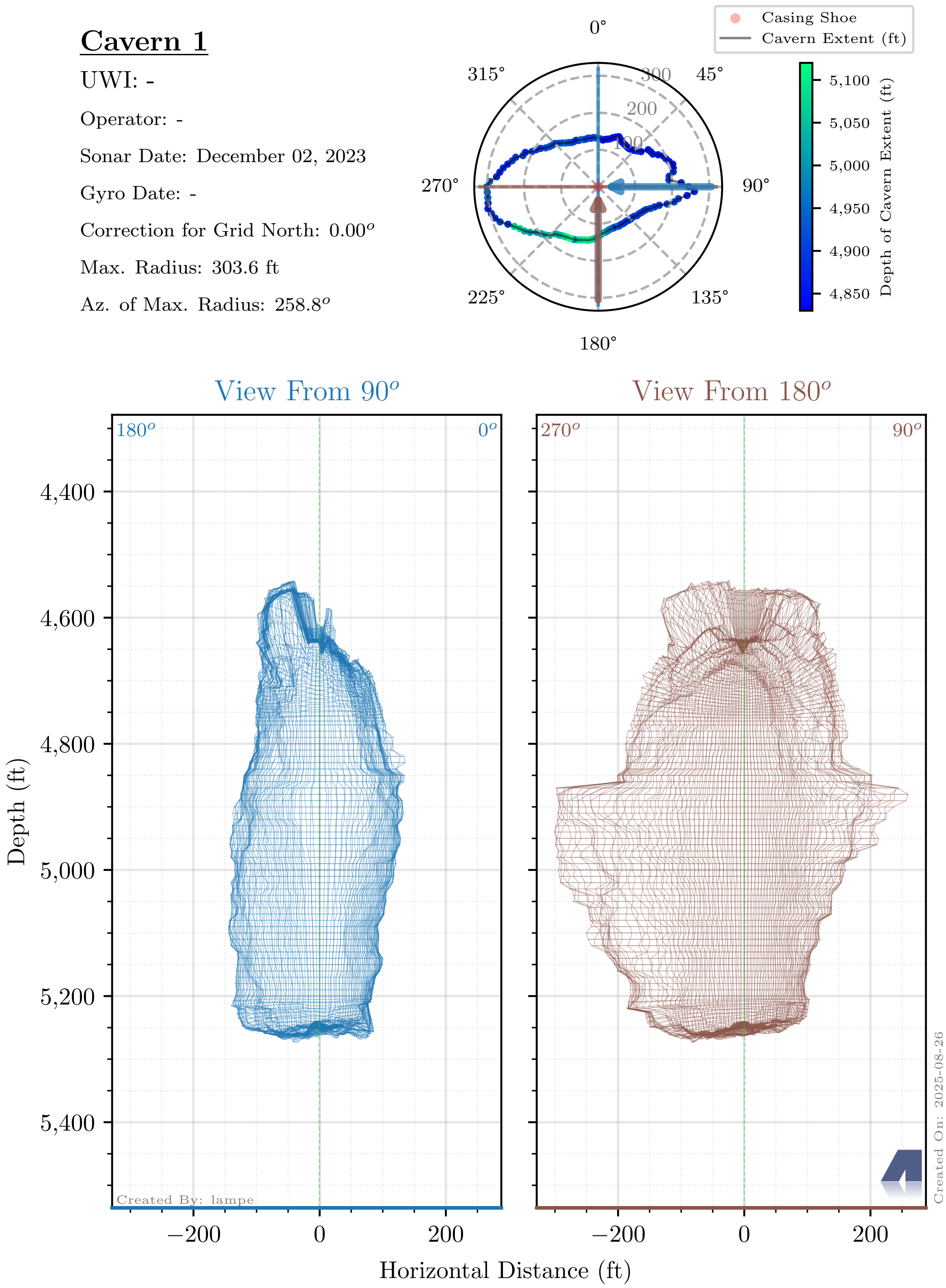

Figure 5: Horizontal extent (top) and vertical cross sections (bottom) from the most recent sonar survey.

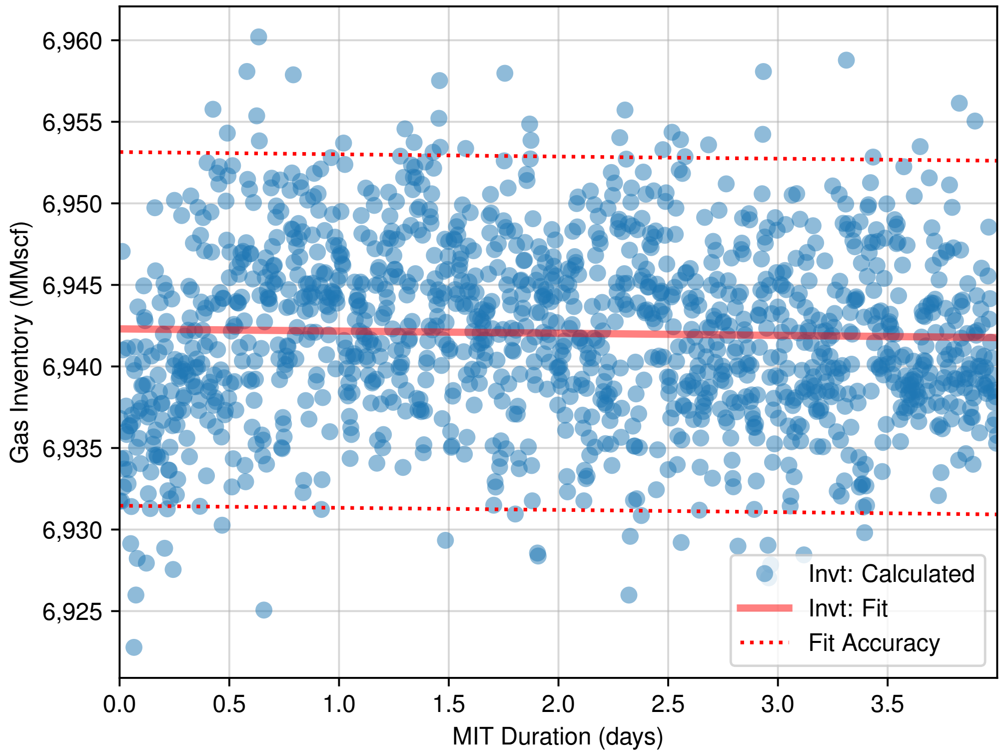

Figure 6: Calculated gas inventory (Invt), fit, and accuracy limits on fit.

3.4 Calculated Gas Inventory

The surface wellhead pressure down-hole temperature were used to calculate gas inventory[1] during the four-day MIT. Results from the 1,343 independent gas-inventory calculations, and the inventory results with time are illustrated in Figure 6. The CLR was determined based on the rate of change of the gas inventory, which was approximated from a linear fit to the inventory with time. The fit accuracy was chosen in terms of a 95% Confidence Interval (95% CI), which is illustrated in Figure 6.

3.5 Assessment of Calculated Leak Rate

The calculated leak rate (CLR) was approximated from a fit to the calculated gas inventory with time. An analysis of the error in the fit was conducted to assess if the residuals were random, and Figure 7 illustrates the distribution of error along with a Gaussian (Normal) curve (shown in red). A fundamental assumption of this analysis was that error in CLR was random. Figure 8 illustrates a probability plot of the CLR residuals along with a straight line, where the R^2 value is approximately unity, which confirms the fitting assumptions [6].

Error in the CLR was determined from the 95% CI associated with the CLR. As depicted in Figure 9, the CLR initially oscillates substantially when there are only a small number of inventory calculations and confidence limits are very large. However, as additional inventory measurements are made and confidence limits become small, the CLR approaches zero. Table 2 provides a summary of the CLR and associated accuracy in terms of MMscf per year (MMscf/yr), thousands of standard cubic feet per day (Mscf/day), barrels per year at average down-hole conditions (B/yr), and standard cubic meters per year (scm/yr).

[1] Gas inventory is presented in terms of million standard cubic feet (MMscf) or million standard cubic meters (MMscm)

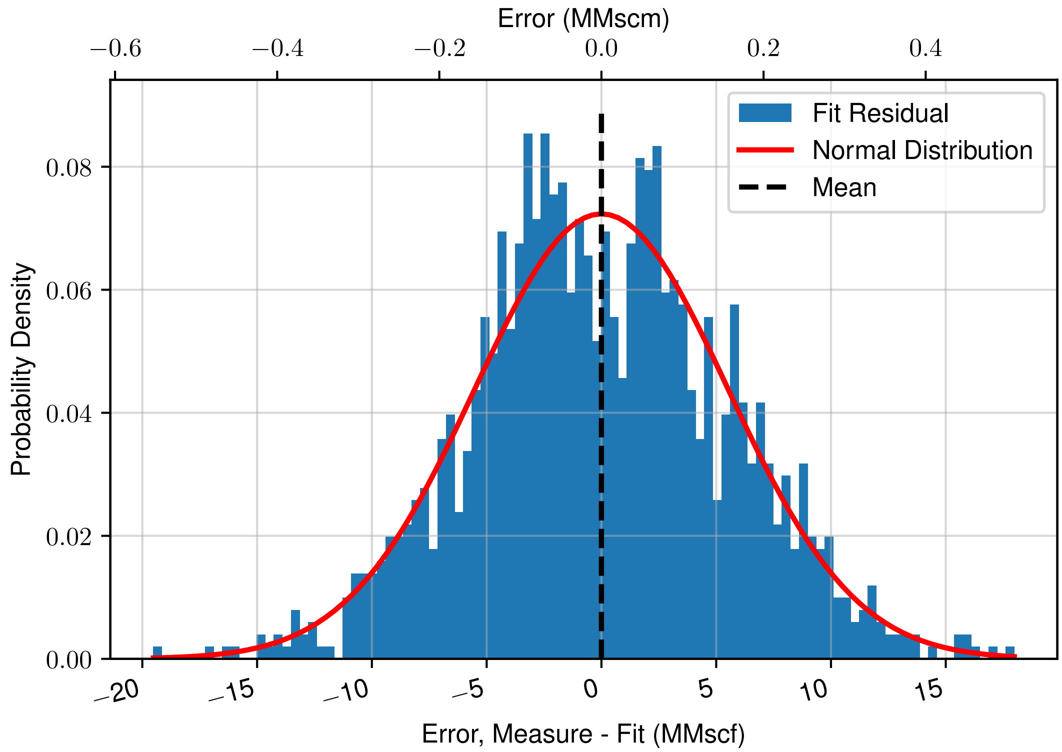

Figure 7: Probability density of the error in the fit to gas inventory.

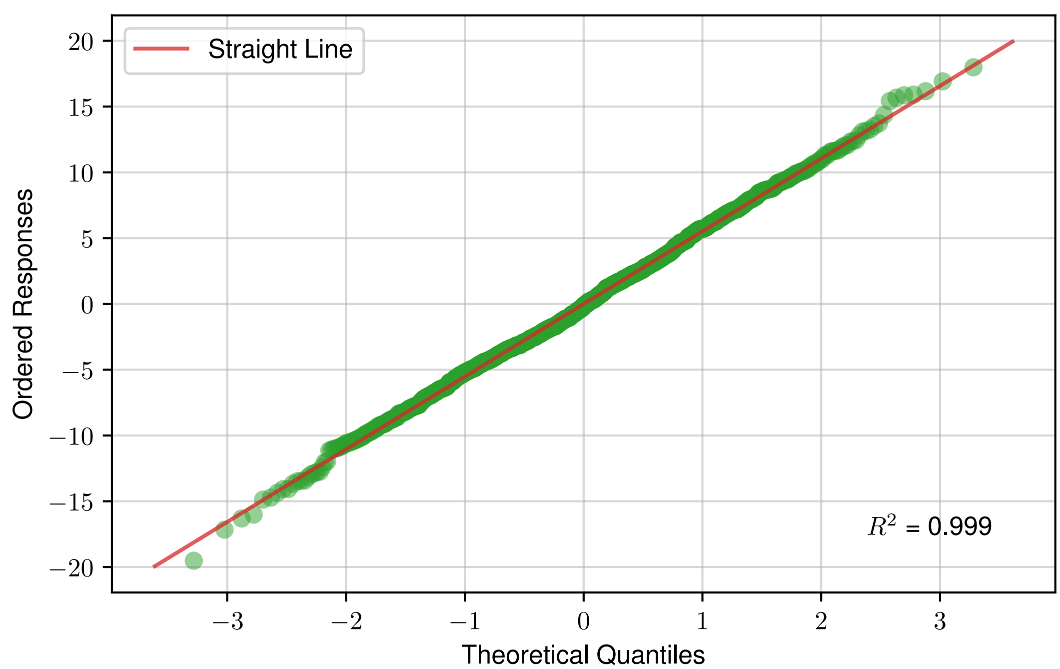

Figure 8: Probability plot of the CLR residuals.

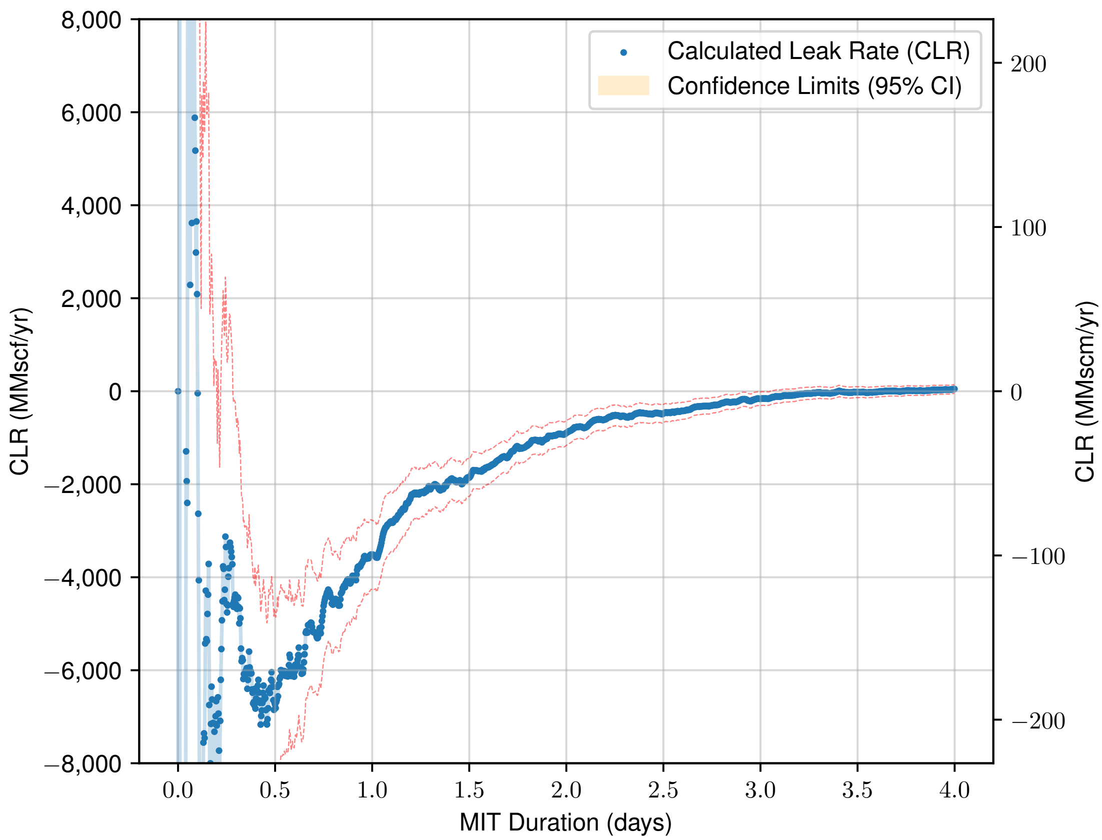

Figure 9: CLR and confidence interval for the MIT.

Table 2: Final values of the CLR and confidence limits (accuracy).

CLR	Accuracy (±)	Units
86.6	103.0	MMscf/yr
237.3	282.2	Mscf/day
146,597	174,359	B/yr
2,452	2,917	10^3 scm/yr

4 Discussion on CLR Accuracy

The technique presented here is applicable for both nitrogen-brine interface MITs and gas-filled MITs. The following discussion highlights the benefits of using optical fiber in both scenarios.

4.1 Nitrogen-Brine Interface MIT

Accuracy of a nitrogen-brine interface MIT is often presented in terms of a Minimum Detectable Leak Rate (MDLR), and Equation 17 provides the commonly used form. Here, $\bar{V}$ is the unit volume at the depth of the gas-brine interface, R is the vertical precision of the logging tool, and t is the duration of the MIT.

$$MDLR = \frac{\bar{V}R}{t} \tag{17}$$

Although the MDLR is the apparent accuracy of the CLR, Equation 17 does not consider most of the parameters used in determining the CLR. The MDLR in this form only provides an estimate of precision when the test fluid density is constant (i.e., the temperature and pressure do not change) and $\bar{V}$ is constant. However, these assumptions are often not valid [7]. Additionally, the vertical resolution of the logging tool (R) is often arbitrarily chosen such that the MIT duration is reduced. Optical fiber (OF) may be suspended at a constant depth during an MIT, which limits the uncertainty associated with error in the log depth. Also, numerous temperature logs may be acquired during an MIT, which allows for a statistical evaluation of CLR accuracy. Therefore, shortcomings of the MDLR calculation can be alleviated with the use of OF.

4.2 Gas-Filled MIT

A common technique for evaluating the accuracy of a gas-filled MIT is to consider the precision of the pressure and temperature acquisition tools. Consider the 4-day MIT discussed in Section 3 and let the CLR accuracy be provided in terms of the following tool calibration:

- pressure: 1.2 psi (8.3 kPa)
- temperature: 1.125 ^{o}F (0.625 ^{o}C)

This approach would result in an MIT accuracy of $\pm$ 7,700 MMscf/yr; which on an annual basis is greater than the entire inventory contained within the cavern (approximately 6,942 MMscf). The MIT error based on tool calibration is approximately 75 times greater than that based on a large number of inventory calculations with OF (provided in Table 2). Therefore, the presented MIT technique allows for a much more accurate characterization of cavern integrity.

4.3 Benefit of Continuous Measurements

The use of OF allows for continuous down-hole measurements that have increased accuracy because:

1. the data acquisition locations are static (i.e., the fiber location is held constant) and
2. a large number of measurements are made over the full cavern height.

Conventional temperature logs are run by lowering sensors from surface to the depth of the test-fluid interface. This results in uncertainty in the logging tool depth that is largely caused by changing line stretch. Because OF is held at a static down-hole depth during the MIT, OF data are not impacted by changing line stretch.

In additional to being held at a constant depth during an MIT, OF has the benefit of being able to acquire large amounts of down-hole data. Confidence in the CLR is only meaningful when a large number of measurements are obtained and statistical methods can be employed. The uncertainty in the CLR decreases in relation to the number of measurements (n) (the relation is $\frac{1}{\sqrt{n}}$). Figure 10 illustrates the relationship between the CLR accuracy and the number of inventory measurements made during the MIT presented in Section 3.

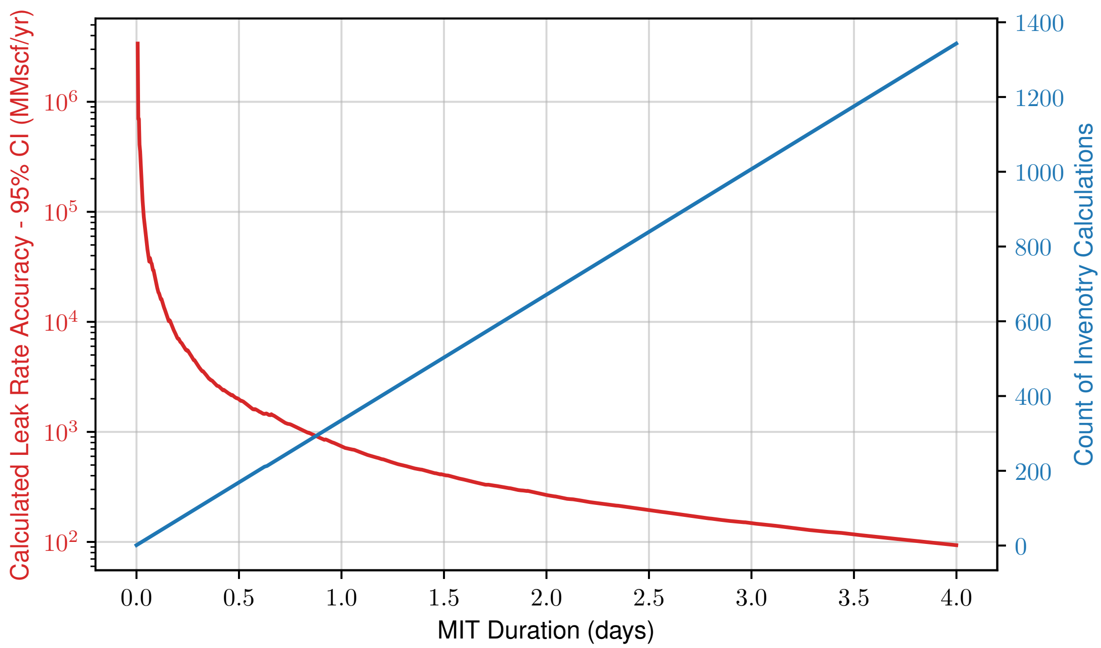

Figure 10: The specific relationship between the number of inventory calculations (blue) and the CLR accuracy (red) for the MIT presented in Section 3.

Additionally, the acquisition of a large number of temperature logs allows for an assessment of thermal stability. Down-hole logs are often run within one or more hanging strings, which results in the logging tool not being in direct contact with the test fluid (as illustrated in Figure 1). Brine temperature within the hanging string may not be representative of the test-fluid outside the hanging string - this results in additional error in the CLR that is often not accounted for. Error in the logged temperature can be minimized by ensuring the down-hole temperatures are stable [7]. Conventional MITs only acquire two sets of temperature logs, which inhibit an accurate assessment of thermal stability. However, the acquisition of continuous down-hole data with OF allows for the an accurate assessment of the temperature, which may be used to assess if the down-hold temperature is stable.

4.4 Shortcomings of Optical Fiber

Optical fiber has many benefits when employed to assess cavern integrity, but challenges do exists. Because data acquired via optical fiber is often distributed (i.e., measurements made along the entire length of the fiber) and continuous (repeated measurements are made during a single logging run) - data from optical fiber are often in HDF5 (Hierarchical Data Format version 5) or other specialized data formats that are suitable for large data sets. This can make assessing the provided data with *standard* software (e.g., Excel) challenging. However, there are many open-source software platforms that provide tools for evaluating DTS and other forms of optical-fiber data.

An additional challenge is the determination of interface depth. Running a conventional nuclear based interface log (e.g., gamma-gamma) is not feasible when there is a string of fiber in the well. Techniques for interpreting interface depths with DTS are in their infancy. Current practice is to positively identify the interface depth prior to initiating an MIT. As analysis techniques mature, the positive identification of interface depths with DTS will become more common.

5 Conclusions

This paper provides theory for conducting an MIT with down-hole data acquired via optical fiber. This technique may be applied to a wide range of MIT scenarios, including a nitrogen-brine interface MIT where the interface is located within the uncased wellbore. The case study presented here described the use of optical fiber for a gas-filled MIT, where the gas-brine interface was located at the cavern floor.

Optical fiber allows for the acquisition of continuous-distributed down-hole temperature data, which when combied with wellhead pressure allows for an accurate characterization of cavern integrity. The large amount data for characterizing the CLR provides increased confidence in the CLR. This is unlike alternative methods for assessing MIT accuracy that provide estimates of CLR precision, such as those based on the interface depth resolution (e.g., MDLR) or the propagation of error.

References

[1] N.E. Van Fossan and F.V. Whelply. "Nitrogen as a Testing Medium for Proving the Mechanical Integrity of Wells". In: *Solution Mining Research Institute Meeting Paper*. Houston, Texas, USA, 1985.

[2] Nils Skaug, Brandon Lampe, and Joe Ratigan. "A Critical Look at the Nitrogen/Brine Interface Mechanical Integrity Test". In: *Solution Mining Research Institute, Technical Conference Paper, Fall*. 2011.

[3] Brandon Schulte, Brandon Lampe, and Ian Welsh. "A Liquid-Liquid Mechanical Integrity Test Ahnalysis That Implements a Fluid Equation of State". In: *Solution Mining Research Institute, Technical Conference Paper, Fall*. 2013.

[4] Arnaud Réveillère. "The development of the concern for tightness in the salt cavern industries, of accurate tightness test techniques and of the concept of Mechanical Integrity Test". PhD thesis. Sorbonne Universitè, Mar. 23, 2023. URL: `https://theses.hal.science/tel-04043152`.

[5] Joseph Nealy, Steve Heath, and Matt Mickelson. "Workover of Domal Cavern Wells Under Gas Pressure Without Snubing". In: *Solution Mining Research Institute, Technical Conference Paper, Fall*. 2024.

[6] John Chambers et al. *Graphical Methods for Data Analysis*. Wadsworth, 1983.

[7] Brandon Lampe and Joe Ratigan. "Pitfalls of a Nitrogen-Brine Interface Mechanical Integrity Test". In: *Solution Mining Research Institute, Technical Conference Paper, Spring*. 2014.